HHS Public Access

Author manuscript

Immunity. Author manuscript; available in PMC 2019 October 03.

Published in final edited form as:

Immunity. 2018 September 18; 49(3): 490–503.e4. doi:10.1016/j.immuni.2018.07.008.

Non-canonical NF-κB Antagonizes STING Sensor-Mediated DNA Sensing in Radiotherapy

Yuzhu Hou[1], **Hua Liang**[1], **Enyu Rao**[1,2], **Wenxin Zheng**[1], **Xiaona Huang**[1], **Liufu Deng**[1,3], **Yuan Zhang**[1], **Xinshuang Yu**[4], **Meng Xu**[1], **Helena Mauceri**[1], **Ainhoa Arina**[1], **Ralph R. Weichselbaum**[1,*], **Yang-Xin Fu**[5,6,*]

[1]Ludwig Center for Metastasis Research, Department of Radiation and Cellular Oncology, The University of Chicago, Chicago, IL 60637, USA

[2]Cancer Institute, Xuzhou Medical University, Xuzhou, Jiangsu, China

[3]Shanghai Institute of Immunology; Department of Immunology and Microbiology, Shanghai Jiao Tong University School of Medicine, China

[4]Department of Radiation Oncology, Shandong Provincial Qianfoshan Hospital, Shandong University, Jinan, China

[5]Department of Pathology, University of Texas Southwestern Medical Center, Dallas, TX 75235-9072, USA

[6]Lead Contact

SUMMARY

The NF-κB pathway plays a crucial role in supporting tumor initiation, progression, and radioresistance of tumor cells. However, the role of the NF-κB pathway in radiation-induced anti-tumor host immunity remains unclear. Here we demonstrated that inhibiting the canonical NF-κB pathway dampened the therapeutic effect of ionizing radiation (IR), whereas non-canonical NF-κB deficiency promoted IR-induced anti-tumor immunity. Mechanistic studies revealed that non-canonical NF-κB signaling in dendritic cells (DCs) was activated by the STING sensor-dependent DNA-sensing pathway. By suppressing recruitment of the transcription factor RelA onto the *Ifnb* promoter, activation of the non-canonical NF-κB pathway resulted in decreased type I IFN expression. Administration of a specific inhibitor of the non-canonical NF-κB pathway enhanced the anti-tumor effect of IR in murine models. These findings reveal the potentially interactive roles for canonical and non-canonical NF-κB pathways in IR-induced STING-IFN production and provide an alternative strategy to improve cancer radiotherapy.

[*]Correspondence: rrw@radonc.uchicago.edu (R.R.W.), yang-xin.fu@utsouthwestern.edu (Y.-X.F.).

AUTHOR CONTRIBUTIONS

Y.H. designed research studies, conducted experiments, and analyzed data. Y.H. and H.L. wrote the manuscript. W.Z. analyzed data; L.D., X.H., E.R., M.X., Y.Z., X.Y., A.A., and H.M. conducted experiments. Y.-X.F. and R.R.W. provided guidance for the research.

SUPPLEMENTAL INFORMATION

Supplemental Information includes five figures and can be found with this article online at https://doi.org/10.1016/j.immuni.2018.07.008.

DECLARATION OF INTERESTS

The authors declare no competing interests.

Graphical Abstract

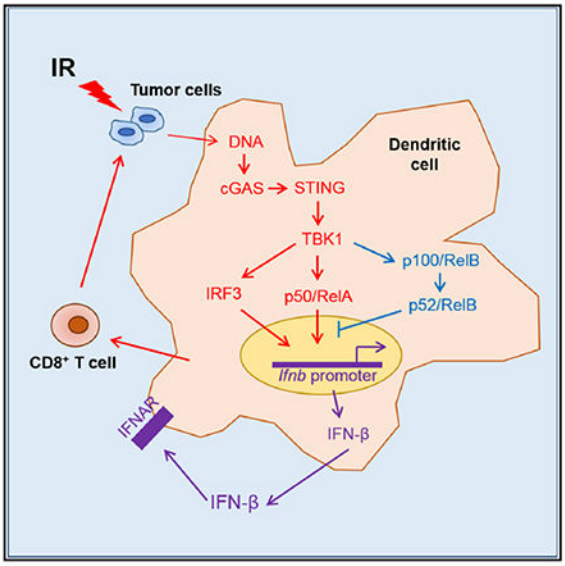

In Brief

It is known that the NF-κB pathway plays a crucial role in supporting tumor initiation, progression, and the radioresistance of tumor cells. Hou et al. demonstrate that the deficiency of non-canonical NF-κB, but not canonical NF-κB, promotes radiation-induced anti-tumor immunity by regulating the STING-mediated type I IFN expression.

INTRODUCTION

Radiotherapy (RT) is widely used as a primary treatment modality for cancer, and the induction of damage to the tumor or to tumor stroma was long thought to be its major mode of action (Prise and O'Sullivan, 2009). Recently, however, increasing evidence demonstrates that ionizing radiation (IR) induces tumor-specific immunity (Reits et al., 2006) and that anti-tumor immunity is required for the full anti-tumor effect of RT (Lee et al., 2009). It is now recognized that the infiltration and priming of $CD8^+$ T cells play a critical role in the efficacy of RT (Lee et al., 2009; Lugade et al., 2005; Takeshima et al., 2010). DCs have been reported to be activated by local IR and required for $CD8^+$ T cell activation and contribute to tumor control by RT (Gupta et al., 2012). These antitumor immune responses have been found to be highly dependent on type I interferon (IFN) signaling (Burnette et al., 2011). Type I IFNs promote dendritic cell (DC) function by stimulating their capacity to process and present antigens as well as to promote DC migration toward lymph nodes (Gardner and Ruffell, 2016; Zitvogel et al., 2015). Stimulator of interferon genes (STING) is an endoplasmic-reticulum-associated protein that activates transcription of the type I IFN gene, via a STING-TBK kinase-IRF3 transcription factor-NF-κB signal transduction pathway (Weichselbaum et al., 2017). Our previous studies demonstrated that STING-dependent cytosolic DNA sensing was required for IR-induced anti-tumor immunity by regulating type I IFN expression (Deng et al., 2014b). However, emerging research also demonstrates that

STING-induced IFN production by IR also promotes innate immune suppression by recruiting monocytic myeloid-derived suppressor cells (MDSCs) into the tumor microenvironment (Liang et al., 2017). Thus, IR not only kills tumor cells directly, but also promotes innate immunity as well as adaptive immune responses via the STING-mediated DNA-sensing pathway. These immune responses induced by IR have important implications for control of localized cancers, as well as control of metastatic disease through the immune-mediated abscopal effect. Therefore, elucidating the interaction of IR and the immune system may have a major impact on cancer treatment.

The mammalian NF-κB family of transcription factors, including RelA, c-Rel, RelB, NF-κB1 (p50 and its precursor p105), and NF-κB2 (p52 and its precursor p100), play a central role in the immune system. The most well-studied activation pathway is the canonical NF-κB pathway, which mainly impinges upon RelA-p50 and c-Rel-p50 heterodimers (Hayden and Ghosh, 2008; Sun, 2012; Vallabhapurapu and Karin, 2009). The activation of the non-canonical NF-κB pathway pivots on activation of RelB-p52 heterodimers in response to a subset of TNF family members, including CD40L, LTαβ, BAFF, RANKL, and TWEAK. In the presence of these ligands, cIAP1 and 2 degrades the TRAF3 ubiquitin ligase and NIK kinase stabilization is achieved. NIK then phosphorylates IKKα and IKKα phosphorylates p100, which is important for the subsequent ubiquitination and partial degradation of p100 by the proteasome to form p52. RelB-p52 heterodimers then translocate into the nucleus to regulate non-canonical NF-κB target genes (Sun, 2012).

The canonical NF-κB signaling pathway has been extensively studied in the context of cancer initiation, progression, and response to RT and chemotherapy (chemo) in both mice and humans (Erstad and Cusack, 2013; Perkins, 2012; Shishodia and Aggarwal, 2004). However, the involvement of the non-canonical NF-κB pathway in cancer biology, and in response to RT, is less well defined. Given that treatment with RT induces NF-κB activation in certain cancer cells and that the activation of NF-κB is associated with the development of radioresistance (Erstad and Cusack, 2013), NF-κB pathways have been considered as a clinical target to counteract radio- and chemo-resistance. However, the role of the interaction of canonical and non-canonical NF-κB pathways in IR-induced anti-tumor immunity is largely unknown. An understanding the role and mechanism of NF-κB in RT may be of great value in designing therapeutic strategies that take advantage of host response in the context of RT.

In this study, we demonstrated that the canonical NF-κB pathway was required for IR-induced anti-tumor immune responses, suggesting that it is not a good therapeutic target to enhance the effect of IR. In contrast, the non-canonical NF-κB pathway negatively regulated RT-induced anti-tumor immunity through STING-dependent DC activation. We demonstrated that irradiated tumor cells activated the non-canonical NF-κB pathway in DCs in a STING-dependent manner and that the activated non-canonical NF-κB pathway controlled the anti-tumor functions of DCs and $CD8^+$ T cells by regulating type I IFN expression. Importantly, inhibition of non-canonical NF-κB signaling with p52-RelB nuclear translocation blockade enhanced the therapeutic effect of RT. Thus, our findings demonstrate that the non-canonical NF-κB pathway inhibits IR-induced innate immune sensing and the

resulting anti-tumor immunity. These findings provide a fresh direction for developing therapeutic strategies targeting NF-κB pathways.

RESULTS

Host Canonical NF-κB Signaling Is Required for IR-Induced Anti-tumor Immunity

To determine whether inhibition of the NF-κB pathway promotes the therapeutic effect of IR, we investigated tumor growth after IR in the presence of JSH-23, a canonical NF-κB pathway inhibitor. JSH-23 abrogated the anti-tumor effect of IR, which suggested that the canonical NF-κB pathway signaling was required for the therapeutic effect of IR (Figures 1A and 1B). Analysis of tumor-infiltrating immune cells profile revealed that the frequency of $CD8^+$ T cells increased in irradiated tumors and decreased in the presence of JSH-23 (Figure 1C). Tumor-infiltrating DCs showed lower MHC-II and CD80 expression in JSH-23-treated mice than control mice (Figures 1D and 1E), which suggested that JSH-23 might alter the antigen-presenting capacity of DCs. Furthermore, our results here indicated that canonical NF-κB pathway inhibition dampened the cross-priming capacity of DCs after RT (Figure 1F). Next, we employed DC-specific RelA-deficient mice *Itgax-cre Rela*$^{f/f}$ and monitored the tumor growth after IR. The results showed that IR controlled tumor growth in control *Rela*$^{f/}$ mice but not in *Itgax-cre Rela*$^{f/f}$ mice, which suggested that RelA deficiency in DCs dampened the anti-tumor effect of IR (Figures 1G and 1H).

Although canonical NF-κB signaling is documented to facilitate radioresistance in tumor cells, our results demonstrated that inhibiting canonical NF-κB dampened the therapeutic effect of RT by regulating IR-induced anti-tumor immunity. The canonical NF-κB pathway signaling in DCs was required for the manifestation of IR-induced therapeutic effects.

Host Non-canonical NF-κB Signaling Deficiency Enhances the Therapeutic Effect of Ionizing Radiation

To investigate the involvement of the non-canonical NF-κB pathway in host response to IR, we employed *Itgax-cre Relb*$^{f/f}$ (DC-deficient) or *Lyz2-cre* (myeloid-deficient) mice which showed no symptoms of autoimmune disease or premature death found in whole body-deficient mice. Using *Relb*$^{f/f}$ mice as controls, we monitored MC38 tumor growth after a single IR dose (20 Gy). The results showed that the anti-tumor effect of RT was enhanced in *Itgax-cre Relb*$^{f/f}$ mice compared with that of *Relb*$^{f/f}$ mice (Figures 2A and S1A). A similar result was observed using a B16-SIY tumor model (Figures S1B and S1C), which suggested that the role of RelB in the anti-tumor effect of RT is not restricted to a specific tumor histology. In contrast, the tumor growth in *Lyz2-cre Relb*$^{f/f}$ mice was comparable with control mice following RT (Figures S1D and S1E), which suggested that RelB in DCs, but not myeloid cells (monocytes, mature macrophages, and granulocytes), plays an inhibitory role in IR-induced tumor control.

RelB is promiscuous in choosing binding partners depending on cell type and stimuli. Instead of its conventional partner, p52, it was reported that RelB could also promote DC activation as a RelB-p50 dimer regulated by the canonical NF-κB pathway (Shih et al., 2012). To determine whether RelB in DCs controls the therapeutic effect of RT through the

non-canonical NF-κB pathway, we employed NF-κB2-deficient (*Nfkb2*$^{-/-}$) mice on a *Rag1*$^{-/-}$ background. This genetic cross allowed us to focus on the role of NF-κB2 in DCs and rule out the effect of intrinsic defects after depletion of NF-κB2 in B cells (Caamaño et al., 1998). T cells were reconstituted by adoptively transferring wild-type CD3^{+} T cells into a *Rag1*$^{-/-}$ background. The resulting tumor growth showed that NF-κB2 deficiency led to enhanced IR response compared with *Nfkb2*$^{+/+}$ mice (Figures 2B and S1F). Together, these data demonstrated that the host non-canonical NF-κB pathway negatively regulates the therapeutic efficiency of RT.

The Non-canonical NF-κB Pathway Negatively Regulates IR-Induced Anti-tumor Immunity

To determine whether IR induces stronger immune responses in mice with deficient non-canonical NF-κB signaling, we analyzed phenotypes and functions of DCs and CD8^{+} T cells in NF-κB2- and Relb-deficient mice after RT. The percentage of CD11c^{+} tumor-infiltrating DCs in *Nfkb2*$^{-/-}$ mice was higher than that of *Nfkb2*$^{+/+}$ mice after IR (Figure S2A). NF-κB2-deficient DCs expressed higher MHC class I and II proteins and the co-stimulatory molecule CD80 (Figure S2B), which suggested more mature and higher cross-priming ability in *Nfkb2*$^{-/-}$ mice. In an ELISPOT cross-priming assay, DCs sorted from tumors grown in *Itgax-cre Relb*$^{f/f}$ and *Nfkb2*$^{-/-}$ mice showed increased priming function compared with control (Figures 2C and S2C). To rule out possible influences from other cell types, the antigen-specific cross-priming ability of bone marrow-derived DCs (BMDCs) were examined. Increased IFN-γ^{+} in wells containing RelB- or NF-κB2-deficient BMDCs (Figures 2D and S2D) suggested that non-canonical NF-κB signaling deficiency intrinsically promoted the antigen processing and presenting capacities of DCs.

The frequency and function of CD8^{+} T cells in tumors grown in *Itgax-cre Re1b*$^{f/f}$ and *Nfkb2*$^{-/-}$ mice also increased compared to those of WT mice after IR. IR enhanced the accumulation of CD45^{+} hematopoietic cells and CD8^{+} T cells among CD45^{+} cells in MC38 tumors grown in WT mice, and to a greater extent, in tumors grown in *Nfkb2*$^{-/-}$ and RelB-deficient mice (Figures S2E, 2E, and S2F). By ELISPOT assay, we observed that IR induced greater CD8^{+} T cell responses against tumor-specific antigen in the TDLN of *Itgax-cre Relb*$^{f/f}$ and *Nfkb2*$^{-/-}$ mice compared with control mice (Figures 2F and S2G). To examine whether increased accumulation and enhanced function of CD8^{+} T cells are relevant to the therapeutic efficacy of RT, we investigated tumor growth in *Relb*$^{f/f}$ and *Itgax-cre Relb*$^{f/f}$ mice in the presence of a CD8^{+} T cell depletion antibody. The enhanced anti-tumor effect of IR in *Itgax-cre Relb*$^{f/f}$ mice and *Nfkb2*$^{-/-}$ mice was abrogated when T cells were not present (Figures 2G and 2H). Taken together, our results demonstrate that non-canonical NF-κB pathway signaling is a negative regulator of anti-tumor immune responses in the context of IR. Deficiency of non-canonical NF-κB signaling in DCs promotes DC function in T cell priming, which in turn leads to an enhanced therapeutic effect of IR.

Non-canonical NF-κB Signaling Deficiency in DCs Promotes IFN-β Expression after IR

We previously demonstrated that the induction of type I IFNs in DCs by IR is essential for functional CD8^{+} T cell-mediated anti-tumor immunity (Burnette et al., 2011; Deng et al., 2014b). To test whether type I IFNs are required for increased anti-tumor effect in mice deficient in non-canonical NF-κB signaling, we blocked type I IFN signaling following IR

with an antibody against IFNAR1. The result showed that the increased anti-tumor effect in *Nfkb2*$^{-/-}$ and *Itgax-cre Relb*$^{f/f}$ mice was abrogated by admin istration of IFNAR1 antibody (Figures 3A and 3B). To test whether the non-canonical NF-κB pathway modulates the anti-tumor functions of DCs and CD8^{+} T cells following IR by regulating type I IFN expression, we measured concentrations of IFN-β protein in tumors. The induction of IFN-β in tumors was increased in *Nfkb2*$^{-/-}$ mice after IR (Figure 3C). We also found that the expression of CXCL10, a type I IFN-stimulated gene, was increased in Nfkb2$^{-/-}$ mice after IR (Figure 3D). To further assess whether the non-canonical NF-κB pathway regulates IFN-β expression in DCs, we measured IFN-β production by BMDCs purified after co-culturing with control or irradiated tumor cells. The amount of secreted IFN-β protein was increased in NF-κB2-defcient BMDCs stimulated with irradiated tumor cells (Figure 3E). We also demonstrated that IFN-β production induced by irradiated tumor cells was increased in BMDCs derived from *Itgaqx-cre Relb*$^{f/f}$ mice compared to that from *Relb*$^{f/f}$ control mice (Figure 3F). Using type I IFN production as readout, we demonstrated that the non-canonical NF-κB pathway is a negative regulator of DC function following IR.

Non-canonical NF-κB Pathway Activation in DCs Is Regulated by the STING-TBK1 Axis after IR

The cGAS-STING pathway plays a critical role in anti-tumor immunity by regulating type I IFN expression (Woo et al., 2014), and our previous studies indicate that STING drives IR-induced anti-tumor immunity by stimulating type I IFN expression (Deng et al., 2014b). Therefore, we investigated whether the non-canonical NF-κB pathway controls STING-mediated type I IFN expression. To address this question, we utilized 5, 6 dimethyl-xanthenone-4-acetic acid (DMXAA), which is a direct ligand for murine STING and induces type I IFN expression in a STING-dependent manner (Corrales et al., 2015; Deng et al., 2014b). While the production of IFN-β by BMDCs was increased by stimulation with DMXAA, IFN-β concentrations were even greater in NF-κB2- and RelB-deficient BMDCs compared with WT controls (Figures 3G and 3H). These data suggested that the non-canonical NF-κB pathway is downstream of STING and therefore able to negate STING action in regulating IR-induced type I IFN expression.

Next, we investigated the activation of STING and non-canonical NF-κB pathways in BMDCs after co-culture with irradiated tumor cells. We found that irradiated tumor cells enhanced the phosphorylation of TBK1 and IRF3 and the activation of non-canonical NF-κB signaling in the BMDCs of WT mice (Figures 4A, 4B, S3A, and S3B). Furthermore, we found that the enhanced activation of non-canonical NF-κB after co-culture with irradiated tumor cells was abolished in STING-deficient BMDCs (Figures 4C and S3C). These results suggested that STING activation is required for IR-induced activation of non-canonical NF-κB signaling in BMDCs. To determine whether STING activation is sufficient to activate non-canonical NF-κB, DMXAA was utilized to stimulate WT- and STING-deficient BMDCs. DMXAA treatment activated nuclear translocation of RelB in a STING-dependent manner (Figures 4D and S3D). As anticipated, TBK1 was also activated by DMXAA in a STING-dependent manner (Figures 4D and S3D). When TBK1 is deficient, DMXAA-induced activation of non-canonical NF-κB was abrogated (Figures 4E and S3E). These

results suggested that TBK1 is a key regulator in STING-induced activation of the non-canonical NF-κB pathway.

To understand whether DNA from irradiated tumor cells is able to trigger the activation of non-canonical NF-κB signaling in DCs through the STING-mediated DNA-sensing pathway in tumor microenvironment, we labeled tumor DNA with EdU before inoculation and detected the up-take of tumor DNA and the activation of STING and non-canonical NF-κB pathways in DCs. As shown in Figure 4F, IR not only increased the up-take of tumor DNA in DCs *in vivo*, but also enhanced phosphorylation of TBK1 and p100 in WT DCs. In contrast, although DCs from STING-deficient mice showed comparable up-take of tumor DNA, the enhanced phosphorylation of TBK1 and p100 was abrogated. These data suggested that IR-induced up-take of tumor DNA in DCs subsequently activated TBK1 and non-canonical NF-κB signaling through the STING pathway.

To dissect which component in the non-canonical NF-κB pathway is the target of STING-TBK1, we examined the activation of up-stream components of the non-canonical NF-κB pathway in BMDCs after stimulation with DMXAA. The degradation of TRAF2 and 3, the accumulation of NIK, and the phosphorylation of IKKα were not altered by DMXAA (Figures 4G and S3F). However, the phosphorylation of p100 (NF-κB2) was increased by DMXAA, suggesting that p100 could be the primary target of STING regulation. By using NF-κB2-defcient BMDCs, we found that p100-p52 was required for nuclear translocation of RelB during STING activation (Figures 4H and S3G). By using BMDCs derived from *Chuk*$^{f/f}$ (*IKKa*) or *Itgax-cre Chuk*$^{f/f}$ mice, our results revealed that activation of non-canonical NF-κB in IKKα-deficient BMDCs by DMXXA was comparable to that in WT cells (Figures 4I and S3H), suggesting that IKKα is dispensable in STING activation of RelB translocation. Furthermore, we observed direct binding between TBK1 and p100 in BMDCs stimulated with DMXAA by using co-IP assay (Figures 4J and S3I). *In vitro* kinase assays showed that WT TBK1, but not TBK1 kinase loss-of-function mutants (including K38A dominant-negative mutation or kinase domain deletion), phosphorylated p100, which suggested that p100 is a substrate of TBK1 (Figure 4K). Taken together, these data suggest that irradiated tumor cells or a STING agonist can activate the STING pathway in DCs, which subsequently activates non-canonical NF-κB signaling in a TBK1-dependent manner.

Non-canonical NF-κB Signaling Regulates IFN-β Expression through Inhibition of RelA Binding to *Ifnb* Promoter in DCs

In antiviral immunity, *Ifnb* expression requires recruitment of a number of transcription factors, including IRF3 and p50-RelA heterodimer, binding to the positive regulatory domains of the *Ifnb* promoter (Jin et al., 2014; Wang et al., 2010). In order to elucidate the mechanism by which non-canonical NF-κB signaling suppresses IR-induced *Ifnb* expression, we examined the activation of IRF3 and canonical NF-κB in BMDCs after co-culturing with irradiated tumor cells. The immunoblotting demonstrated that irradiated MC38 cells promoted the nuclear translocation of both IRF3 and RelA in BMDCs (Figures 5A and S4A). Similarly, the STING agonist, DMXAA, also enhanced the phosphorylation of IκBα and the nuclear translocation of RelA in a time-dependent manner (Figures 5B and S4B). Furthermore, the activation of IRF3 and canonical NF-κB signaling in DCs was both

STING and TBK1 dependent, as indicated by diminished activation in Tmem173- or Tbk1-deficient cells (Figures 5C, 5D, S4C, and S4D). The activation of these components are required for IR-induced *Ifnb* expression in BMDCs when co-cultured with irradiated tumor cells or stimulated by a STING agonist; as in cells deficient in Tbk1 (Figures 5E and S4E), Irf3 (Figures 5F and S4E), or Rela (Figures 5G and S4G), IFN-β production was abrogated. Inhibition of the canonical NF-κB pathway by JSH-23 also showed similar results (Figures 5H and S4H). These data suggest that both the TBK1-IRF3 and canonical NF-κB pathways are required for IR-induced *Ifnb* expression in DCs.

To understand how non-canonical NF-κB signaling negatively regulates type I IFN induction, we examined the effect of non-canonical NF-κB deficiency on STING-induced activation of signaling and transcriptional factors involved in *Ifnb* expression. The loss of NF-κB2 did not affect DMXAA-induced activation of either the TBK1-IRF3 or canonical NF-κB pathways, suggesting that the NF-κB2 pathway does not directly regulate the STING-TBK1-IRF3 axis (Figures 5I and S4I). Next we asked whether non-canonical NF-κB signaling suppressed type I IFN expression by inhibiting STING-induced transcriptional factors binding to the *Ifnb* promoter by Chromatin immunoprecipitation (ChIP) assays. The results showed that the binding of RelB to the *Ifnb* promoter was increased by DMXAA treatment in WT BMDCs, but not in NF-κB2-deficient cells (Figure 5J). Additionally, the binding of RelA to the *Ifnb* promoter was increased by DMXAA treatment in WT BMDCs, which was further elevated markedly in NF-κB2-deficient cells (Figure 5K). In contrast, the DMXAA-induced binding of IRF3 to the *Ifnb* promoter was comparable between WT and NF-κB2-deficient BMDCs (Figure 5L). These data suggest that non-canonical NF-κB signaling negatively regulates IR-induced type I IFN production by inhibiting binding of RelA to the *Ifnb* promoter without having an effect on the binding ability of IRF3.

To further explore the relationship between canonical and non-canonical NF-κB signaling in regulating the anti-tumor effect of IR, we monitored the tumor growth in *Itgax-cre Relb*$^{f/f}$ mice in the presence of JSH-23. The result showed that the enhanced anti-tumor effect in *Itgax-cre Relb*$^{f/f}$ mice was abrogated by JSH-23, which suggested that canonical NF-κB was required for an enhanced anti-tumor effect in RelB-deficient mice (Figures 2A and S4J). Furthermore, canonical NF-κB signaling in DCs contributed to the anti-tumor effect of IR by inducing IFN-β, since administration of exogenous IFN-β restored the anti-tumor effect of IR in *Itgax-cre Rela*$^{f/f}$ mice (Figures 1G and S4K).

Inhibition of Non-canonical NF-κB Signaling Can Promote IR-Induced Anti-tumor Immunity

To further investigate the role of non-canonical NF-κB signaling in the context of the clinical response of human cancer patients, we analyzed overall survival of patients receiving RT for glioblastoma (GBM) in a publicly available database (The Cancer Genome Atlas [TCGA]); we found that patients with low *Nfkb2* expression had better overall survival after RT (Figure S5A). A similar result was obtained when the overall survival was analyzed based on the *Relb* expression (Figure S5B). These results suggest that non-canonical NF-κB signaling diminishes the therapeutic effect of IR not only in pre-clinical tumor models, but also in patient clinical response.

We hypothesize that the inhibition of the non-canonical NF-κB pathway may be used as a translational strategy to enhance RT-induced anti-tumor effects. To address this question, we employed a competitive inhibitor (SN52) of NF-κB2 (Xu et al., 2008), which inhibits the nuclear translocation of p52-RelB heterodimers. SN52, but not SN52Mu (a mutant control for SN52), inhibited DMXAA-induced nuclear translocation of RelB in BMDCs (Figure S5C). In contrast, treatment with SN52 did not change the activation of canonical NF-κB signaling. Furthermore, we found that nuclear translocation of RelB was increased in DCs isolated from irradiated tumors, and this activation was abolished by SN52 intratumoral (i.t.) treatment (Figure S5D). Consistent with the results of NF-κB2-deficient cells, inhibition of non-canonical NF-κB by SN52 increased *Ifnb* expression in BMDCs stimulated with irradiated tumor cells or STING agonist (Figures 6A and S5E). These results demonstrate that SN52 can effectively recapitulate the phenotype of non-canonical NF-κB deletion, resulting in alleviation of the negative regulation on IR- or STING-induced IFN-β production. To test the efficacy of SN52 *in vivo*, we administrated SN52Mu and SN52 i.t. immediately after IR. The combination of SN52 and IR enhanced anti-tumor immune functions of both DCs (Figure 6B) and $CD8^+$ T cells (Figure 6C) and subsequently reduced tumor burden (Figures 6D and S5F) more effectively compared with IR alone, suggesting that non-canonical NF-κB inhibition can potentiate the anti-tumor effect of IR. We next tested whether the combination of IR and SN52 produced an abscopal effect by using a contralateral tumor model, in which the primary tumors were treated with IR and/or SN52 and the secondary tumors did not receive any treatment. A growth delay was observed in the IR+SN52 group but not in groups receiving either treatment alone (Figure 6E). These results suggested that non-canonical NF-κB inhibition also promoted systemic anti-tumor immunity induced by IR. To further test whether SN52 promoted the therapeutic effect of IR through the STING-IFNs axis, we investigated tumor growth in STING-deficient mice (Figure 6F) and in the presence of IFNAR1-blocking antibody (Figure 6G) following treatment with IR and/or SN52. The results indicated that STING and type I IFNs were required for SN52-enhanced anti-tumor effects of RT.

Although SN52 promoted the therapeutic effect of IR by regulating type I IFNs, the tumors that received combination treatment were not completely eliminated. Sustained IFN-I signaling induces immunosuppressive mechanisms, including the expression of both PD-L1 on DCs and other myeloid cells and PD-1 on T cells, which result in $CD8^+$T cell exhaustion (Garcia-Diaz et al., 2017; Tang et al., 2018). Therefore, we treated tumor-bearing mice with anti-PD-L1 after SN52 and IR treatment. PD-L1 blockade enhanced the therapeutic effect of the SN52+IR combination (Figure 6H) and led to tumor rejection (Figure S5G). To address whether this combination treatment resulted in generation of prolonged protective T cell immunity, tumor-free mice were rechallenged with higher dose of MC38 tumor cells on the opposite flank. No palpable tumors were detected on the treated mice after a few weeks (Figure 6I). Together, combining IR with manipulation of the STING-IFN pathway and checkpoint inhibition for better innate priming and alleviation of immunosuppression may present a fresh avenue for cancer therapy.

DISCUSSION

Radiation induces both innate and adaptive anti-tumor immune responses, and the axis of DCs and CTLs plays a crucial role in this process (Gupta et al., 2012; Lee et al., 2009). Type I IFNs induced by IR are essential for both cross-presentation capacity of dendritic cells and anti-tumoral function of $CD8^+$ T cells (Burnette et al., 2011; Zitvogel et al., 2015). Our previous work established that the cGAS- and STING-dependent cytosolic DNA-sensing pathways in DCs are required for type I IFN induction after IR (Deng et al., 2014b). In this report, we identify a previously unknown downstream control mechanism of the DNA-sensing pathway in DCs that has particular relevance to cancer therapy. Our data demonstrate that the innate DNA-sensing pathway not only exerts immunostimulatory functions via IFN production, but also activates the non-canonical NF-κB pathway, which in turn negatively regulates type I IFN induction after IR. These results describe an alternative mechanism of STING regulation and indicates that targeting the non-canonical NF-κB pathway enhanced anti-tumor effects of IR.

We found that irradiated tumor cells stimulated the activation of the non-canonical NF-κB pathway in DCs in a STING-TBK1-dependent manner. Activation of the STING pathway was both necessary and sufficient for the activation of the non-canonical NF-κB pathway. The stabilization of NIK and phosphorylation of IKKα are well known as central early steps in activation of non-canonical NF-κB pathway (Vallabhapurapu and Karin, 2009). Jin et al. (2012) found that TBK1 controls IgA class switching in B cells by negatively regulating phosphorylation and subsequent degradation of NIK. Cytosolic DNA can activate the non-canonical NF-κB pathway in a STING-dependent and TBK1-independent manner in MEFs or human tumor cells (Abe and Barber, 2014; Bakhoum et al., 2018). However, our data demonstrated that DMXAA, a STING agonist, did not increase the accumulation of NIK or phosphorylation of IKKα in the process of activating p100 phosphorylation and nuclear translocation of p52-RelB heterodimers. Rather, our results suggest that in response to IR-induced damage, host immune cells may preferentially use the cGAS-STING DNA-sensing pathway, instead of NIK-IKKα, to activate the non-canonical NF-κB pathway. Understanding this alternative regulation would be of value for choosing or designing inhibitors of the non-canonical NF-κB pathway to enhance the therapeutic effect of IR as well as therapies in virus infection and auto-immune diseases. It is intriguing that activation of the STING pathway induced both the canonical (triggering production of IFN) and the non-canonical (inhibiting IFN production) NF-κB pathways in DCs. This may represent an intricate and complex regulation of IFN production responding to differential stimuli.

A growing body of evidence shows that the canonical NF-κB pathway plays a crucial role in supporting tumor initiation and progression via mechanisms including stimulating cell proliferation, inhibiting apoptosis (Beg and Baltimore, 1996), increasing metastasis (Wang et al., 1999), and angiogenesis (Koch et al., 1992). Radiation induces constitutive canonical NF-κB activation in certain cancers (Brach et al., 1991; Chen et al., 2002), and activation of NF-κB is associated with the development of radioresistance. Given this evidence, a large number of inhibitors of canonical NF-κB pathway are undergoing development and some have been tested in clinical trials. However, the anti-tumor efficacy and toxicity of these inhibitors are not promising. In our present study, an inhibitor of the canonical NF-κB

pathway decreased the therapeutic effect of IR by suppressing IR-induced anti-tumor immune response. Specifically, canonical NF-κB, together with IRF3, is required for the induction of type I IFN in DCs stimulated by irradiated tumor cells through STING-TBK1 signaling. Taken together, the canonical NF-κB pathway may not be an ideal target for promoting the therapeutic effect of IR because of its differential roles in inducing tumor radioresistance and its requirement for IR-induced anti-tumor immunity. Similar to the canonical NF-κB pathway, non-canonical NF-κB is also known as a tumor-promoting factor due to its role in regulating the expression of BIM, BMF (Vallabhapurapu et al., 2015), and BCL2 (Wang et al., 2007) in tumor cells. In addition, non-canonical NF-κB signaling in tumor cells is reported to be activated by IR and mediates radioresistance by regulating the expression of MnSOD (Josson et al., 2006), Survivin, and BCL2 (Mineva et al., 2009). However, we found that, in contrast to canonical NF-κB, the non-canonical NF-κB pathway in DCs negatively regulates IR-induced anti-tumor immunity by controlling type I IFN expression. Consistently, we found that non-canonical NF-κB inhibition, but not canonical NF-κB inhibition, promoted tumor regression induced by local IR. We have previously shown that, in some tumors, intrinsic radiobiological properties of the tumor cells are less important than the immune microenvironments (Liang et al., 2013) and, in this context, inhibiting the non-canonical NF-κB pathway may be particularly important. Our findings reveal a molecular mechanism of IR-mediated anti-tumor immunity through an alternative model of STING regulation and provide insight into therapeutic strategies targeting the NF-κB pathway in cancer immunotherapy.

STAR★METHODS

CONTACT FOR REAGENT AND RESOURCE SHARING

Further information and requests for resources and reagents should be directed to and fulfilled by the Lead Contact, Dr. Yang-Xin Fu (yang-xin.fu@utsouthwestern.edu).

EXPERIMENTAL MODEL AND SUBJECT DETAILS

***In vivo* Animal Studies—**C57BL/6J wild-type (WT), *Itgax-cre+-Tg, Rela*$^{f/f}$ mice were purchased from Jackson Laboratory. *Nfkb2*$^{-/-}$ mice were provided by Dr. Ulrich Siebenlist, NIAID, NIH. *Chuk*$^{f/f}$ mice were kindly provided by Dr. Yinling Hu, NCI, NIH. *Relb*$^{f/f}$ mice were kindly provided by Dr. Falk Weih, Forschungszentrum Karlsruhe, Germany. *Irf3*$^{-/-}$ mice were kindly provided by T. Taniguchi of University of Tokyo. *Tmem173*$^{-/-}$ mice were kindly provided by Dr. Glen N. Barber of University of Miami School of Medicine and backcrossed to B6 background for 8 times in our lab. All experimental groups included randomly chosen female littermates of ages around 8 weeks and of the same strain. All the mice were maintained and used in accordance to the animal experimental guidelines set by the Institute of Animal Care and Use Committee of the University of Chicago.

Cell Lines—Single-cell suspensions of bone marrow cells were obtained from C57BL/6J, *Nfkb2*$^{-/-}$, *Itgax-cre Relb*$^{f/f}$, *Itgax-cre Chuk*$^{f/f}$, *Tmem173*$^{-/-}$, and *Irf3*$^{-/-}$ mice. The cells were cultured in RPMI-1640 medium containing 10% FBS (DENVILLE), supplemented with 20 ng/ml GM-CSF. Fresh media with GM-CSF was added into culture on day 3. BMDCs were harvested for stimulation assay on day 7. *Tbk1*$^{+/+}$ and *Tbk1*$^{-/-}$ macrophages were kindly

provided by Dr. Leticia Corrales of University of Chicago. MC38, MC38-SIY and B16-SIY tumor cell lines were kindly provided by Dr. Xuanming Yang of University of Chicago and grown in DMEM medium containing 10% FBS, at 37°C and 5% CO_2.

METHOD DETAILS

Tumor Growth and Treatments—1×10^6 MC38, MC38-SIY or B16-SIY tumor cells were subcutaneously injected into the flank of mice. Tumors were measured and irradiated at 20 Gy as described in (Deng et al., 2014a). To reconstitute T cell deficiency in *Rag1*$^{-/-}$ background, 1×10^7 wild-type $CD3^+$ T cells were adoptively transferred into $Rag1^{-/-}Nfkb2^{-/-}$ and *Rag1*$^{-/-}$ mice immediately prior to irradiation. For type I IFN blockade experiments, 200 mg anti-IFNAR1 mAb was intratumorally injected on day 0 and 2 after radiation. For $CD8^+$ T cell depletion experiments, 200 mg anti-CD8 mAb was delivered 4 times by i.p. injection every 3 days starting 1 day before radiation. For JSH-23 treatment experiments, 6 mg/kg JSH-23 was given by gavage daily starting 1 day before IR for totally 14 days. For SN52 treatment experiments, 40 mg SN52 was administered for 4 times by i.t. injection every 2 days starting 1 day before radiation and same amount of SN52Mu was used as control. For anti-PD-L1 treatment experiments, 200 μg anti-PD-L1 (10F.9G2) or isotype control were given by i.p. every three days for a total of four times starting on the day of IR.

Flow Cytometry—Tumor tissues were cut into small pieces and digested by 1 mg/ml collagenase IV (Sigma) and 0.2 mg/ml DNase I (Sigma) for 1 hr at 37°C. Suspension cells were blocked with anti-FcR (2.4G2, BioXcell) and then stained with fluorescence-labeled antibodies against CD11c, I-Ab, H-2Kb, CD80, CD86, CD8 and CD45.2. Flow cytometry were performed on BD LSRFortessa at core facility of University of Chicago and data were analyzed with FlowJo software. For up-taking of tumor DNA test, MC38 tumor cells were labeled with 10 mM EdU (Click-iT Plus EdU Alexa Fluor 647 Flow Cytometry Assay Kit) overnight and inoculated into mice (4×10^6 cells/mouse). The next day, tumors were harvested and EdU and phoshpo-TKB1 or -p100 was analyzed by flow cytometry.

***In Vitro* Culture and Function Assay of BMDCs—**8×10^6 MC38-SIY cells were plated into 10 cm cell culture dishes overnight, and then pretreated with 40 Gy and incubated for 12 hr. BMDCs were added and co-cultured with MC38-SIY cells at the ratio of 1:1 in the presence of fresh GM-CSF for an additional 6–8 hr. Subsequently purified $CD11c^+$ cells with EasySep Mouse CD11c Positive Selection Kit II (STEMCELL) were incubated with isolated $CD8^+$ T cells from naive 2C mice for 3 days (Figure S3A). For IFN-β detection, 1×10^6 cells/ml purified $CD11c^+$ cells from co-culture were seeded into 96-well plates and the supernatants were harvested after 3 day incubation (Figure S3B).

Measurement of IFNγ-Secreting $CD8^+$ T Cells by ELISPOT Assay—2×10^4 purified $CD11c^+$ cells were incubated with $CD8^+$ T cells isolated from naive 2C mice (EasySep Mouse CD8a Positive Selection Kit (STEMCELL)) for 3 days at the ratio of 1:10. For tumor-specific CD8+T cells functional assay, MC38 tumor cells were exposed to 20 ng/ml murine IFNγ for 24 hr prior to plating with purified $CD8^+$ T from DLN. 2×10^5 $CD8^+$ T cells were incubated with MC38 at the ratio of 10:1 for 48 hr. ELISPOT assays

were performed to detect the cytokine spots of IFN-γ according to product protocol (Millipore).

ELISA—Tumor tissues were homogenized in PBS with protease inhibitor followed by addition of Triton X-100. Cell culture supernatants were obtained from isolated $CD11c^+$ cells after 48 hr-incubation with fresh GM-CSF. The concentration of IFN-β and CXCL10 was measured with VeriKine-HS Mouse Interferon Beta Serum ELISA Kit (PBL Assay Science) and mouse CXCL10 Quantikine ELISA kit (R&D) in accordance with the manufacturer's instructions, respectively.

Western Blot Analysis—Whole-cell protein was extracted with Triton X-100 buffer (150 mM sodium chloride, 50 mM Tris, 1% Triton X-100; pH 8.0) with proteinase inhibitors and phosphatase inhibitors (Thermo Scientific). Cytoplasmic (CE) and nuclear (NE) protein were extracted with NE-PER Nuclear and Cytoplasmic Extraction Reagents (Thermo Scientific). Immuno-blotting analyses were performed as previously described (Hou et al., 2014). The amount of loaded protein was normalized to GAPDH mAb (Proteintech Group) or HDAC1 mAb (Cell Signaling).

Chromatin Immunoprecipitation Assays—BMDCs (2×10^7) were stimulated with 50 μg/ml DMXAA for 1 hr, flowed by fixation with 1% formaldehyde and sonication as previously described (Nelson et al., 2006). Lysates were subjected to immunoprecipitation with the indicated antibodies or control IgG, and the precipitated DNA was then purified by Magna ChIP A/G Chromatin Immunoprecipitation Kit (Millipore) and quantified by qPCR via a pair of primers that amplify the PRDIII-II region of the *Ifnb* promoter (forward: 5′-ATTCCTCTGAGGCAGAAAGGACCA-3′; reverse: 5′-GCAAGATGAGGCAAAGGCTGTCAA-3′). Input DNA was used as an internal control and the data are shown as the relative fold increased over IgG control.

Immunoprecipitation Assays—WT BMDCs (2×10^7) were treated with 20 μM MG132 for 15 min followed by stimulating of 50 mg/ml DMXAA for indicated time. Cell lysates were subjected to immunoprecipitation with 2 μg indicated antibodies by using Pierce Crosslink Magnetic Co-IP Kit (ThermoFisher). The protein level in eluted supernatant were detected by using indicated antibodies with Western Blot.

***In vitro* Kinase Assays—**pCDNA3.1 vectors containing His-tagged TBK1 WT (wild-type), TBK1 K38A (Lys38 mutated to Ala), TBK1 KDD (kinase domain deletion) and HA-tagged wild-type p100 were purchased from GenScript. Recombinant proteins were expressed in HEK293 cells and purified with His-tag and HA-tag isolation kits from Invitrogen and Thermo Scientific. *In vitro* kinase activities were analyzed by reading the generation of ADP with Universal Kinase Activity Kit from R&D Systems.

QUANTIFICATION AND STATISTICAL ANALYSIS

Analyses were performed using GraphPad Prism software 6. Data were analyzed by one-way ANOVA with Tukey's Multiple Comparison Test or Student's t test. P values < 0.05 were considered statistically significant.

Supplementary Material

Refer to Web version on PubMed Central for supplementary material.

ACKNOWLEDGMENTS

The authors would like to thank Amy K. Huser for editing assistance and Rolando Torres for assistance in animal studies. This research was supported in part by Mr. & Mrs. Vincent Foglia, The Chicago Tumor Institute, an endowment from the Ludwig Cancer Research Foundation to R.R.W., and NIH grant NCI-R21 CA195075 to R.R.W. This work was in part supported by the NIH grant CA134563 to Y.-X.F. and by Cancer Prevention and Research Institute of Texas grant RR150072 to Y.-X.F. Flow cytometry cost was covered in part by University of Chicago Cancer Center Support Grant (P30CA014599).

REFERENCES

Abe T, and Barber GN (2014). Cytosolic-DNA-mediated, STING-dependent proinflammatory gene induction necessitates canonical NF-κB activation through TBK1. J. Virol 88, 5328–5341. [PubMed: 24600004]

Bakhoum SF, Ngo B, Laughney AM, Cavallo JA, Murphy CJ, Ly P, Shah P, Sriram RK, Watkins TBK, Taunk NK, et al. (2018). Chromosomal instability drives metastasisthrough a cytosolic DNA response. Nature 553, 467–472. [PubMed: 29342134]

Beg AA, and Baltimore D (1996). An essential role for NF-kappaB in preventing TNF-alpha-induced cell death. Science 274, 782–784. [PubMed: 8864118]

Brach MA, Hass R, Sherman ML, Gunji H, Weichselbaum R, and Kufe D (1991). Ionizing radiation induces expression and binding activity ofthe nuclear factor kappa B. J. Clin. Invest 88, 691–695. [PubMed: 1864978]

Burnette BC, Liang H, Lee Y, Chlewicki L, Khodarev NN, Weichselbaum RR, Fu YX, and Auh SL (2011). The efficacy of radiotherapy relies upon induction oftype i interferon-dependent innate and adaptive immunity. Cancer Res. 71, 2488–2496. [PubMed: 21300764]

Caamaño JH, Rizzo CA, Durham SK, Barton DS, Raventós-Suárez C, Snapper CM, and Bravo R (1998). Nuclearfactor(NF)-kappa B2 (p100/p52) is required for normal splenic microarchitecture and B cell-mediated immune responses. J. Exp. Med 187, 185–196. [PubMed: 9432976]

Chen X, Shen B, Xia L, Khaletzkiy A, Chu D, Wong JY, and Li JJ (2002). Activation of nuclear factor kappaB in radioresistance ofTP53-inactive human keratinocytes. Cancer Res. 62, 1213–1221. [PubMed: 11861406]

Corrales L, Glickman LH, McWhirter SM, Kanne DB, Sivick KE, Katibah GE, Woo SR, Lemmens E, Banda T, Leong JJ, et al. (2015). Direct activation of STING in the tumor microenvironment leads to potent and systemic tumor regression and immunity. Cell Rep. 11, 1018–1030. [PubMed: 25959818]

Deng L, Liang H, Burnette B, Beckett M, Darga T, Weichselbaum RR, and Fu YX (2014a). Irradiation and anti-PD-L1 treatment synergistically promote anti-tumor immunity in mice. J. Clin. Invest 124, 687–695. [PubMed: 24382348]

Deng L, Liang H, Xu M, Yang X, Burnette B, Arina A, Li XD, Mauceri H, Beckett M, Darga T, et al. (2014b). STING-dependent cytosolic DNA sensing promotes radiation-induced type I interferon-dependent anti-tumor immunity in immunogenic tumors. Immunity 41, 843–852. [PubMed: 25517616]

Erstad DJ, and Cusack JC Jr. (2013). Targeting the NF-κB pathway in cancer therapy. Surg. Oncol. Clin. N. Am 22, 705–746. [PubMed: 24012396]

Garcia-Diaz A, Shin DS, Moreno BH, Saco J, Escuin-Ordinas H, Rodriguez GA, Zaretsky JM, Sun L, Hugo W, Wang X, et al. (2017). Interferon receptor signaling pathways regulating PD-L1 and PD-L2 expression. Cell Rep. 19, 1189–1201. [PubMed: 28494868]

Gardner A, and Ruffell B (2016). Dendritic cells and cancer immunity. Trends Immunol. 37, 855–865. [PubMed: 27793569]

Gupta A, Probst HC, Vuong V, Landshammer A, Muth S, Yagita H, Schwendener R, Pruschy M, Knuth A, and van den Broek M (2012). Radiotherapy promotes tumor-specific effector CD8+ T cells via dendritic cell activation. J. Immunol 189, 558–566. [PubMed: 22685313]

Hayden MS, and Ghosh S (2008). Shared principles in NF-kappaB signaling. Cell 132, 344–362. [PubMed: 18267068]

Hou Y, Lin H, Zhu L, Liu Z, Hu F, Shi J, Yang T, Shi X, Guo H, Tan X, et al. (2014). The inhibitory effect of IFN-g on protease HTRA1 expression in rheumatoid arthritis. J. Immunol 193, 130–138. [PubMed: 24907345]

Jin J, Xiao Y, Chang JH, Yu J, Hu H, Starr R, Brittain GC, Chang M, Cheng X, and Sun SC (2012). The kinaseTBK1 controls IgAclass switching by negatively regulating non-canonical NF-κB signaling. Nat. Immunol 13, 1101–1109. [PubMed: 23023393]

Jin J, Hu H, Li HS, Yu J, Xiao Y, Brittain GC, Zou Q, Cheng X, Mallette FA, Watowich SS, and Sun SC (2014). Non-canonical NF-κB pathway controls the production of type I interferons in antiviral innate immunity. Immunity 40, 342–354. [PubMed: 24656046]

Josson S, Xu Y, Fang F, Dhar SK, St Clair DK, and St Clair WH (2006). RelB regulates manganese superoxide dismutase gene and resistance to ionizing radiation of prostate cancer cells. Oncogene 25, 1554–1559. [PubMed: 16261162]

Koch AE, Polverini PJ, Kunkel SL, Harlow LA, DiPietro LA, Elner VM, Elner SG, and Strieter RM (1992). Interleukin-8 as a macrophage-derived mediator of angiogenesis. Science 258, 1798–1801. [PubMed: 1281554]

Lee Y, Auh SL, Wang Y, Burnette B, Wang Y, Meng Y, Beckett M, Sharma R, Chin R, Tu T, et al. (2009). Therapeutic effects of ablative radiation on local tumorrequireCD8+T cells: changing strategiesfor cancer treatment. Blood 114, 589–595. [PubMed: 19349616]

Liang H, Deng L, Chmura S, Burnette B, Liadis N, Darga T, Beckett MA, Lingen MW, Witt M, Weichselbaum RR, and Fu YX (2013). Radiation-induced equilibrium is a balance between tumor cell proliferation and T cell-mediated killing. J. Immunol 190, 5874–5881. [PubMed: 23630355]

Liang H, Deng L, Hou Y, Meng X, Huang X, Rao E, Zheng W, Mauceri H, Mack M, Xu M, et al. (2017). Host STING-dependent MDSC mobilization drives extrinsic radiation resistance. Nat. Commun 8, 1736–1746. [PubMed: 29170400]

Lugade AA, Moran JP, Gerber SA, Rose RC, Frelinger JG, and Lord EM (2005). Local radiation therapy of B16 melanoma tumors increases the generation of tumor antigen-specific effector cells that traffic to the tumor. J. Immunol 174, 7516–7523. [PubMed: 15944250]

Mineva ND, Wang X, Yang S, Ying H, Xiao ZX, Holick MF, and Sonenshein GE (2009). Inhibition of RelB by 1,25-dihydroxyvitamin D3 promotes sensitivity of breast cancer cells to radiation. J. Cell. Physiol 220, 593–599. [PubMed: 19373868]

Nelson JD, Denisenko O, and Bomsztyk K (2006). Protocol for the fast chromatin immunoprecipitation (ChIP) method. Nat. Protoc 1, 179–185. [PubMed: 17406230]

Perkins ND. (2012). The diverse and complex roles of NF-κB subunits in cancer. Nat. Rev. Cancer 12, 121–132. [PubMed: 22257950]

Prise KM, and O'Sullivan JM (2009). Radiation-induced bystander signalling in cancer therapy. Nat. Rev. Cancer 9, 351–360. [PubMed: 19377507]

Reits EA, Hodge JW, Herberts CA, Groothuis TA, Chakraborty M, Wansley EK, Camphausen K, Luiten RM, de Ru AH, Neijssen J, et al. (2006). Radiation modulates the peptide repertoire, enhances MHC class I expression, and induces successful anti-tumor immunotherapy. J. Exp. Med 203, 1259–1271. [PubMed: 16636135]

Shih VF, Davis-Turak J, Macal M, Huang JQ, Ponomarenko J, Kearns JD, Yu T, Fagerlund R, Asagiri M, Zuniga EI, and Hoffmann A (2012). Control of RelBduring dendritic cell activation integrates canonical and non-canonical NF-κB pathways. Nat. Immunol 13, 1162–1170. [PubMed: 23086447]

Shishodia S, and Aggarwal BB (2004). Nuclearfactor-kappaB: afriend ora foe in cancer? Biochem. Pharmacol 68, 1071–1080. [PubMed: 15313403]

Sun SC (2012). The non-canonical NF-κB pathway. Immunol. Rev 246, 125–140. [PubMed: 22435551]

Takeshima T, Chamoto K, Wakita D, Ohkuri T, Togashi Y, Shirato H, Kitamura H, and Nishimura T (2010). Local radiation therapy inhibits tumor growth through the generation oftumor-specific CTL: its potentiation by combination with Th1 cell therapy. Cancer Res. 70, 2697–2706. [PubMed: 20215523]

Tang H, Liang Y, Anders RA, Taube JM, Qiu X, Mulgaonkar A, Liu X, Harrington SM, Guo J, Xin Y, et al. (2018). PD-L1 on host cells is essential for PD-L1 blockade-mediated tumor regression. J. Clin. Invest 128, 580–588. [PubMed: 29337303]

Vallabhapurapu S, and Karin M (2009). Regulation and function of NF-kappaB transcription factors in the immune system. Annu. Rev. Immunol 27, 693–733. [PubMed: 19302050]

Vallabhapurapu SD, Noothi SK, Pullum DA, Lawrie CH, Pallapati R, Potluri V, Kuntzen C, Khan S, Plas DR, Orlowski RZ, et al. (2015). Transcriptional repression by the HDAC4-RelB-p52 complex regulates multiple myeloma survival and growth. Nat. Commun 6, 8428. [PubMed: 26455434]

Wang W, Abbruzzese JL, Evans DB, and Chiao PJ (1999). Overexpression of urokinase-type plasminogen activator in pancreatic adenocarcinoma is regulated by constitutively activated RelA. Oncogene 18, 4554–4563. [PubMed: 10467400]

Wang X, Belguise K, Kersual N, Kirsch KH, Mineva ND, Galtier F, Chalbos D, and Sonenshein GE (2007). Oestrogen signalling inhibits invasive phenotype by repressing RelB and its target BCL2. Nat. Cell Biol 9, 470–478. [PubMed: 17369819]

Wang J, Basagoudanavar SH, Wang X, Hopewell E, Albrecht R, Garcia-Sastre A, Balachandran S, and Beg AA (2010). NF-kappaB RelA subunit is crucial for early IFN-beta expression and resistance to RNA virus replication. J. Immunol 185, 1720–1729. [PubMed: 20610653]

Weichselbaum RR, Liang H, Deng L, and Fu YX (2017). Radiotherapy and immunotherapy: a beneficial liaison? Nat. Rev. Clin. Oncol 14, 365–379. [PubMed: 28094262]

Woo SR, Fuertes MB, Corrales L, Spranger S, Furdyna MJ, Leung MY, Duggan R, Wang Y, Barber GN, Fitzgerald KA, et al. (2014). STING-dependent cytosolic DNA sensing mediates innate immune recognition of immunogenic tumors. Immunity 41, 830–842. [PubMed: 25517615]

Xu Y, Fang F, St Clair DK, Sompol P, Josson S, and St Clair WH (2008). SN52, a novel nuclear factor-kappaB inhibitor, blocks nuclear import of RelB:p52 dimer and sensitizes prostate cancer cells to ionizing radiation. Mol. Cancer Ther 7, 2367–2376. [PubMed: 18723484]

Zitvogel L, Galluzzi L, Kepp O, Smyth MJ, and Kroemer G (2015). Type I interferons in anticancer immunity. Nat. Rev. Immunol 15, 405–414. [PubMed: 26027717]

Highlights

- Canonical NF-κB pathway is required for radiation-induced anti-tumor immunity
- Non-canonical NF-κB deficiency promotes anti-tumor immunity after radiotherapy
- Non-canonical NF-κB pathway inhibits radiation-induced STING-mediated type I IFNs
- Inhibiting non-canonical NF-κB pathway potentiates the therapeutic effect of radiation

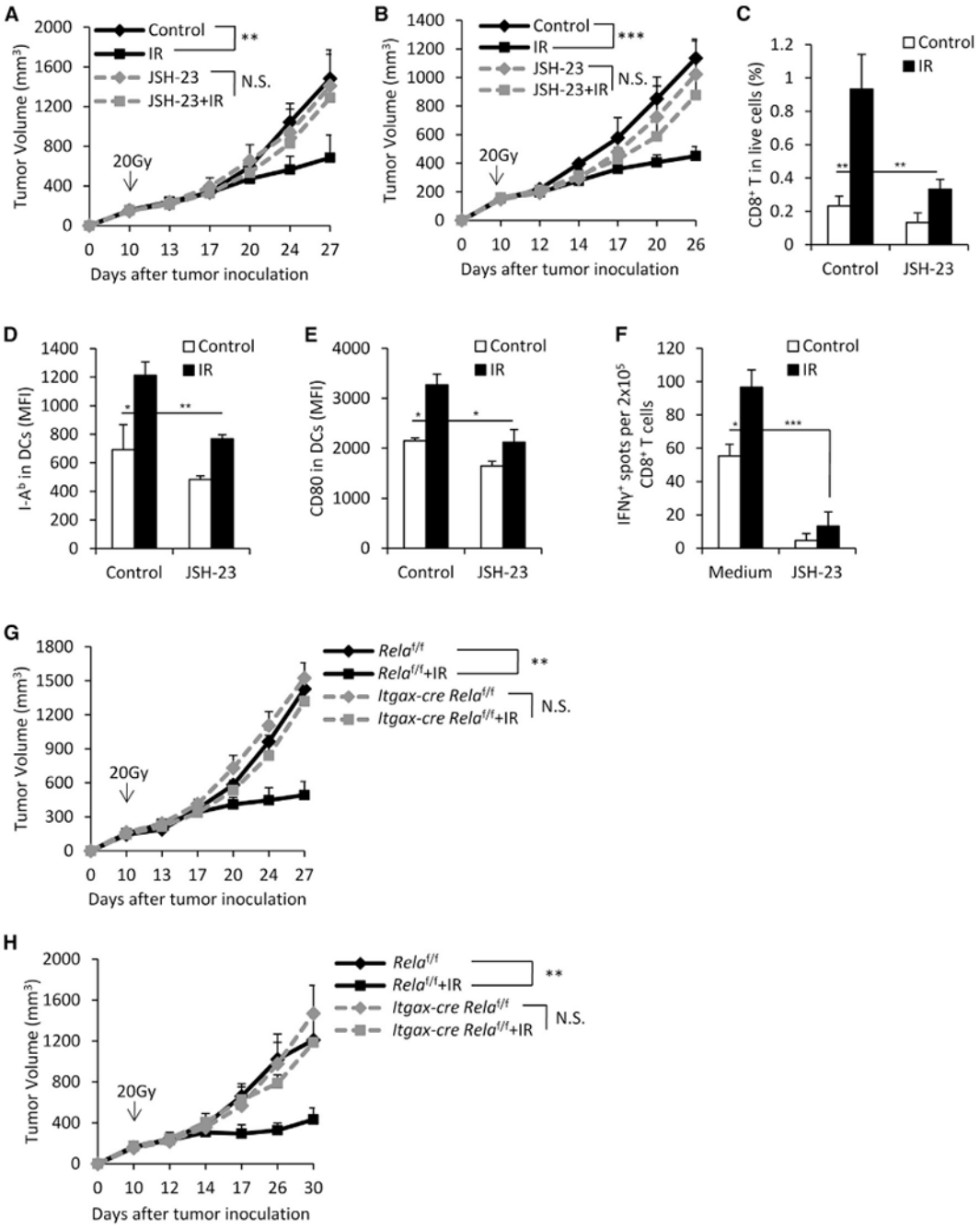

Figure 1. Host Canonical NF-κB Is Required for Anti-tumor Immunity Induced by Ionizing Radiation

(A–E) B6 mice were inoculated s.c. with MC38 cells (A, C, D, and E) or B16-SIY cells (B) on day 0. On day 10, tumors received one dose of 20 Gy ionizing radiation (IR) and 6 mg/kg JSH-23 was given by gavage daily starting 1 day before radiation for 14 days.

(A and B) Tumor growth was monitored after radiation.

(C) Seven days after IR, tumors were removed and digested. The frequency of $CD8^+$ T cells in tumor was analyzed by flow cytometry.

(D and E) Four days after IR, tumors were removed and digested. The expressions of I-A^b (D) and CD80 (E) on $CD45^+CD11c^+$ DCs were analyzed by flow cytometry.

(F) BMDCs were co-cultured with irradiated or non-irradiated MC38-SIY cells in presence or absence of 25 μM JSH-23. After 6–8 hr, $CD11c^+$ DCs were isolated and co-cultured with $CD8^+$ T cells from naive 2C mice for 3 days and the cross-priming activity of BMDCs were analyzed by ELISPOT assays.

(G and H) *Rela*$^{f/f}$ mice and *Itgax-cre Rela*$^{f/f}$ mice were inoculated with MC38 cells (G) or B16-SIY cells (H) on day 0. On day 10, tumors received one dose of 20 Gy IR. Tumor growth was monitored after radiation.

Representative data are shown from three experiments (one experiment for B and H) conducted with 4–5 mice per group. Data are represented as mean ± SD; *$p < 0.05$, **$p < 0.01$, and ***$p < 0.001$.

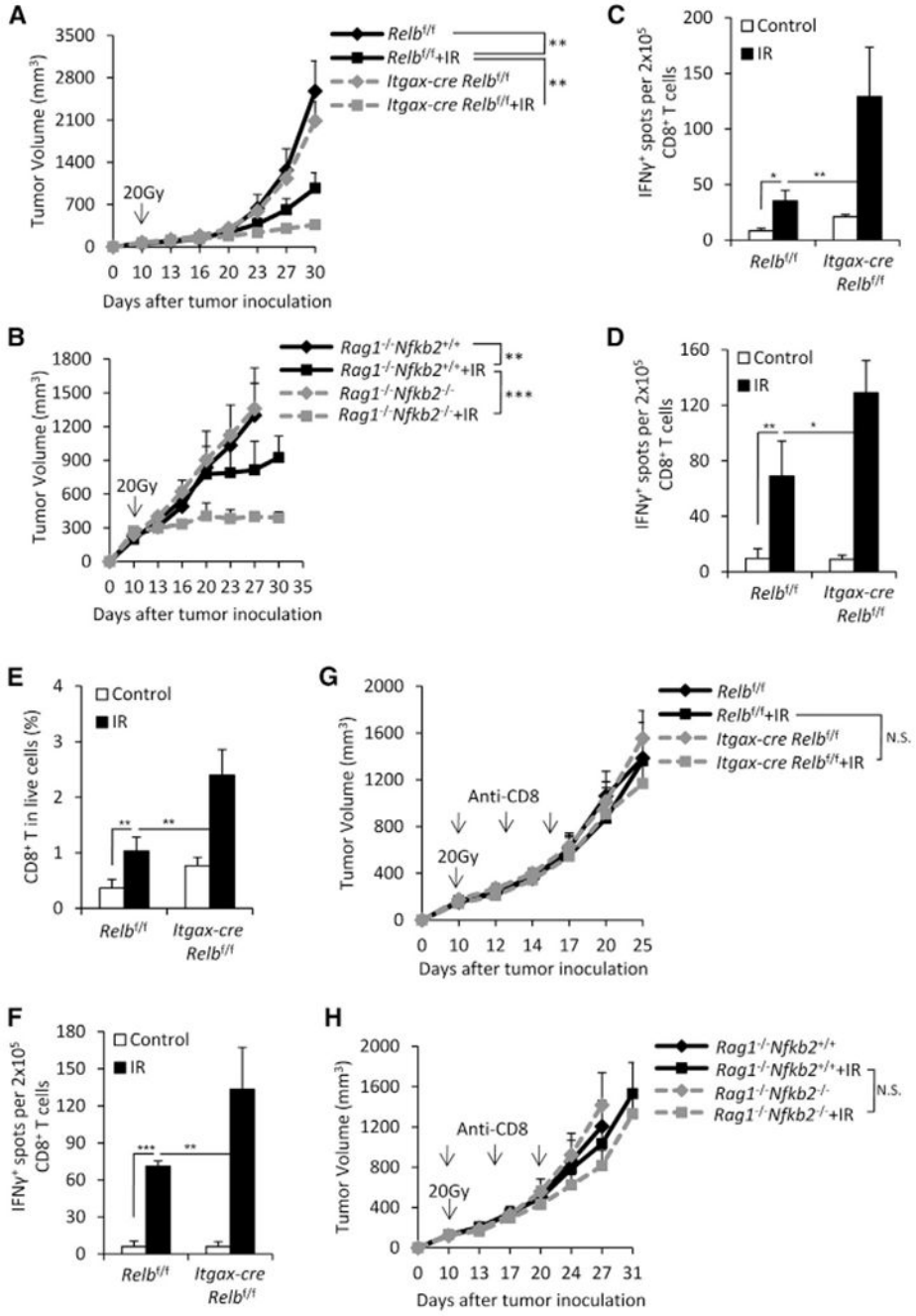

Figure 2. Non-canonical NF-κB Deficiency Enhances Adaptive Immunity via Augmenting DC Priming Function after IR

(A) *Relb*$^{f/f}$ mice and *Itgax-cre Relb*$^{f/f}$ mice were inoculated with MC38 cells on day 0. On day 10, tumors locally received one dose of 20 Gy IR. Tumor growth was monitored after radiation.

(B) *Nfkb2*$^{+/+}$ and *Nfkb2*$^{-/-}$ mice, bred to *Rag1*$^{-/-}$ background, were inoculated with MC38 cells on day 0. On day 10, tumors locally received one dose of 20 Gy IR and the mice were transferred i.v. with 1×10^7 $CD3^+$ T cells isolated from naive WT mice. Tumor growth was monitored after radiation.

(C) MC38-SIY tumor model were established in *Relb*$^{f/f}$ mice and *Itgax-cre Relb*$^{f/f}$ mice and treated with IR as described in (A). On day 4 post IR, tumors were removed and digested. The CD11c^{+} DCs were sorted and then co-cultured with CD8^{+} T cells from naive 2C mice for 3 days and the cross-priming activity of tumor infiltrating DCs were analyzed by ELISPOT assays.

(D) BMDCs from *Relb*$^{f/f}$ mice and *Itgax-cre Relb*$^{f/f}$ mice were used for co-culture with irradiated or non-irradiated MC38-SIY cells. Subsequently cross-priming activity of purified BMDCs was analyzed by ELISPOT assays as described in Figure 1F.

(E–G) MC38 tumor model were established in *Relb*$^{f/f}$ mice and *Itgax-cre Relb*$^{f/f}$ mice and treated with IR as described in (A).

(E) On day 7 post IR, tumors were removed and the frequency of infiltrating CD8^{+} T cells was analyzed by flow cytometry.

(F) On day 7 post IR, tumor-draining lymph nodes (TDLNs) were removed and digested. Tumor antigen-specific CD8^{+} T cell function was measured by ELISPOT assays by co-culturing purified TDLN CD8^{+} cells with IFN-γ-treated MC38 tumor cells.

(G) 200 μg anti-CD8 mAb was administered i.p. in tumor bearing mice every 3 days for a total of three times starting from the day of radiation.Tumor growth was monitored after radiation.

(H) *Nfkb2*$^{+/+}$ and *Nfkb2*$^{-/-}$ mice were inoculated with MC38 cells and treated with IR and T cell transfer as described in (B). 200 μg anti-CD8 mAb was administered as described in (G). Tumor growth was monitored after radiation.

Representative data are shown from three experiments (one experiment for G) conducted with 4–5 mice per group. Data are represented as mean ± SD; *$p < 0.05$, **$p < 0.01$, and ***$p < 0.001$. Please also see Figures S1 and S2.

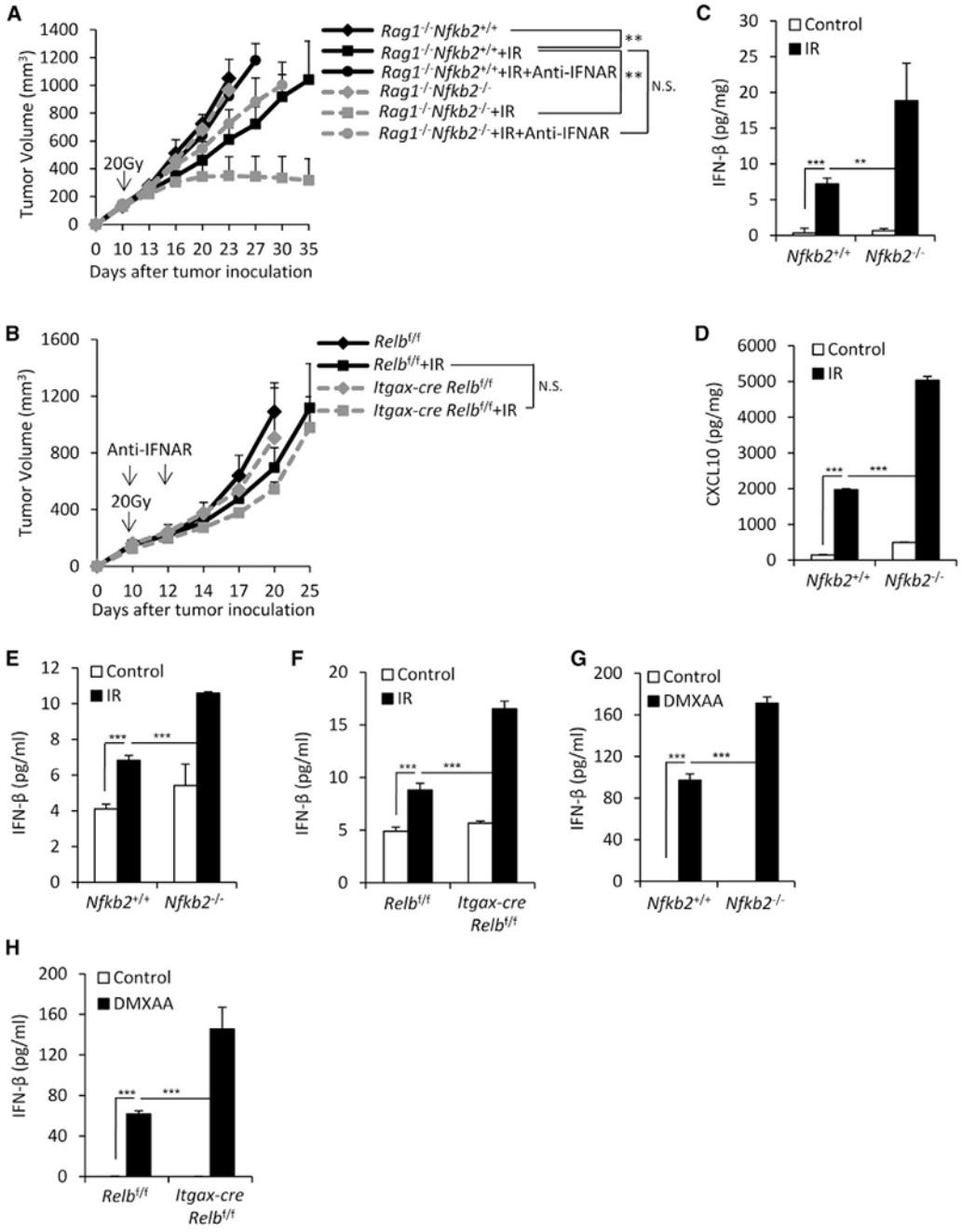

Figure 3. Non-canonical NF-κB Deficiency in DCs Promote IFN-β Expression after Irradiation

(A and B) MC38 tumor model were established in *Nfkb2*$^{+/+}$ and *Nfkb2*$^{-/-}$ mice (A) or *Relb*$^{f/f}$ and *Itgax-cre Relb*$^{f/f}$ (B) mice and treated with IR as described in Figures 2B and 2A. 200 μg anti-IFNAR1 was administered intratumorally on days 0 and 2 after radiation. Tumor growth was monitored after radiation.

(C and D) Tumors were removed 3 days after radiation and homogenized in PBS with protease inhibitor. ELISA assay was performed to measure IFN-γ (C) and CXCL10 (D).

(E and F) BMDCs derived from *Nfkb2*$^{+/+}$ and *Nfkb2*$^{-/-}$ mice (E) or *Relb*$^{f/f}$ and *Itgax-cre* *Relb*$^{f/f}$ mice (F) were co-cultured with irradiated or non-irradiated MC38 cells. The purified CD11c^{+} cells were incubated for additional 3 days and supernatants were collected to measure IFN-β by ELISA assay.

(G and H) BMDCs derived from *Nfkb2*$^{+/+}$ and *Nfkb2*$^{-/-}$ mice (G) or *Relb*$^{f/f}$ and *Itgax-cre* *Relb*$^{f/f}$ mice (H) were stimulated with 50 μg/mL DMXAA for 24 hr. The amount of IFN-β in supernatants was measured by ELISA.

Representative data are shown from three experiments (one experiment for B) conducted with 4–5 (A, B) or 3–4 (C–H) mice per group. Data are represented as mean ± SD; **$p < 0.01$ and ***$p < 0.001$.

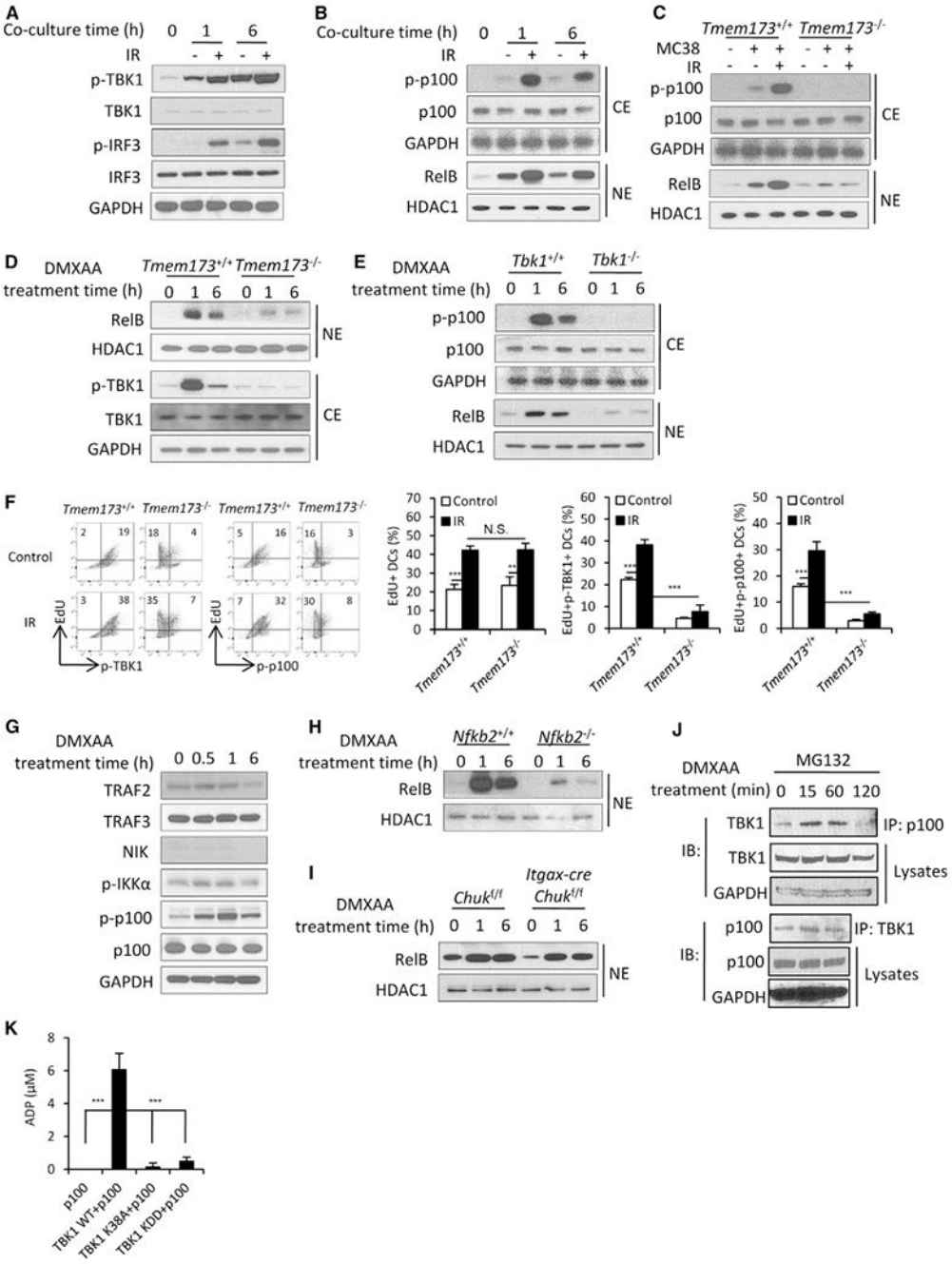

Figure 4. Irradiated Tumor Cells Promote Non-canonical NF-κB Activation in DCs in a STING-TBK1-Dependent Manner

(A and B) Immuno-blotting analysis of indicated phosphorylated (p-) and total protein in whole-cell lysates (A) or cytoplasmic (CE) and nuclear (NE) extracts (B) of purified BMDCs after co-cultured with irradiated or non-irradiated MC38 cells for indicated time. (C) Immuno-blotting analysis of indicated phosphorylated (p-) and total protein in cytoplasmic (CE) and nuclear (NE) extracts of purified *Tmem17*$^{+/+}$ and *Tmem173*$^{-/-}$ BMDCs after co-cultured with irradiated or non-irradiated MC38 cells for 1 hr.

(D) Immuno-blotting analysis of indicated phosphorylated (p-) and total protein in cytoplasmic (CE) and nuclear (NE) extracts of *Tmem17*$^{+/+}$ and *Tmem173*$^{-/-}$ BMDCs stimulated with 50 μg/mL DMXAA for indicated time.

(E) Immuno-blotting analysis of indicated phosphorylated (p-) and total protein in cytoplasmic (CE) and nuclear (NE) extracts of *Tbk1*$^{+/+}$ and *Tbk1*$^{-/-}$ macrophages after stimulated with 50 μg/mL DMXAA for indicated time points.

(F) MC38 cells were labeled with EdU and inoculated into mice and the tumor bumps were irradiated with 20 Gy. The next day, tumor bumps were harvested and digested into single-cell suspensions. Cells were fixed, permeabilized, and stained with indicated antibodies. The frequency of EdU^{+}, EdU^{+} p-TBK1^{+}, and EdU^{+} p-p100^{+} cells in live CD45^{+}CD11c^{+} DCs were analyzed by flow cytometry.

(G) Immuno-blotting analysis of indicated protein in whole-cell lysates of BMDCs after being stimulated with 50 μg/mL DMXAA for indicated time points.

(H) Immuno-blotting analysis of indicated protein in nuclear (NE) extracts of *Nfkb2*$^{+/+}$ and *Nfkb2*$^{-/-}$ BMDCs after being stimulated with 50 μg/mL DMXAA for indicated time points.

(I) Immuno-blotting analysis of indicated protein in nuclear (NE) extracts of BMDCs derived from *Chuk*$^{f/f}$ and *Itgax-cre Chuk*$^{f/f}$ mice after being stimulated with 50 μg/mL DMXAA for indicated time points.

(J) WT BMDCs were stimulated with 50 μg/mL DMXAA for indicated time in presence of 20 μM MG132. Whole-cell lysates were subjected to p100 or TBK1 followed by detecting p100 or TBK1 associated TBK1 or p100 by immuno-blotting.

(K) *In vitro* kinase assay of TBK1 WT, K38A (Lys38 mutated to Ala), and KDD (kinase domain depletion) on substrate p100. The rate of ADP production was detected to reflect the kinetics of the kinase reaction.

Representative data are shown from three experiments (one experiment for K). Data are represented as mean ± SD; ***$p < 0.001$. Please also see Figure S3.

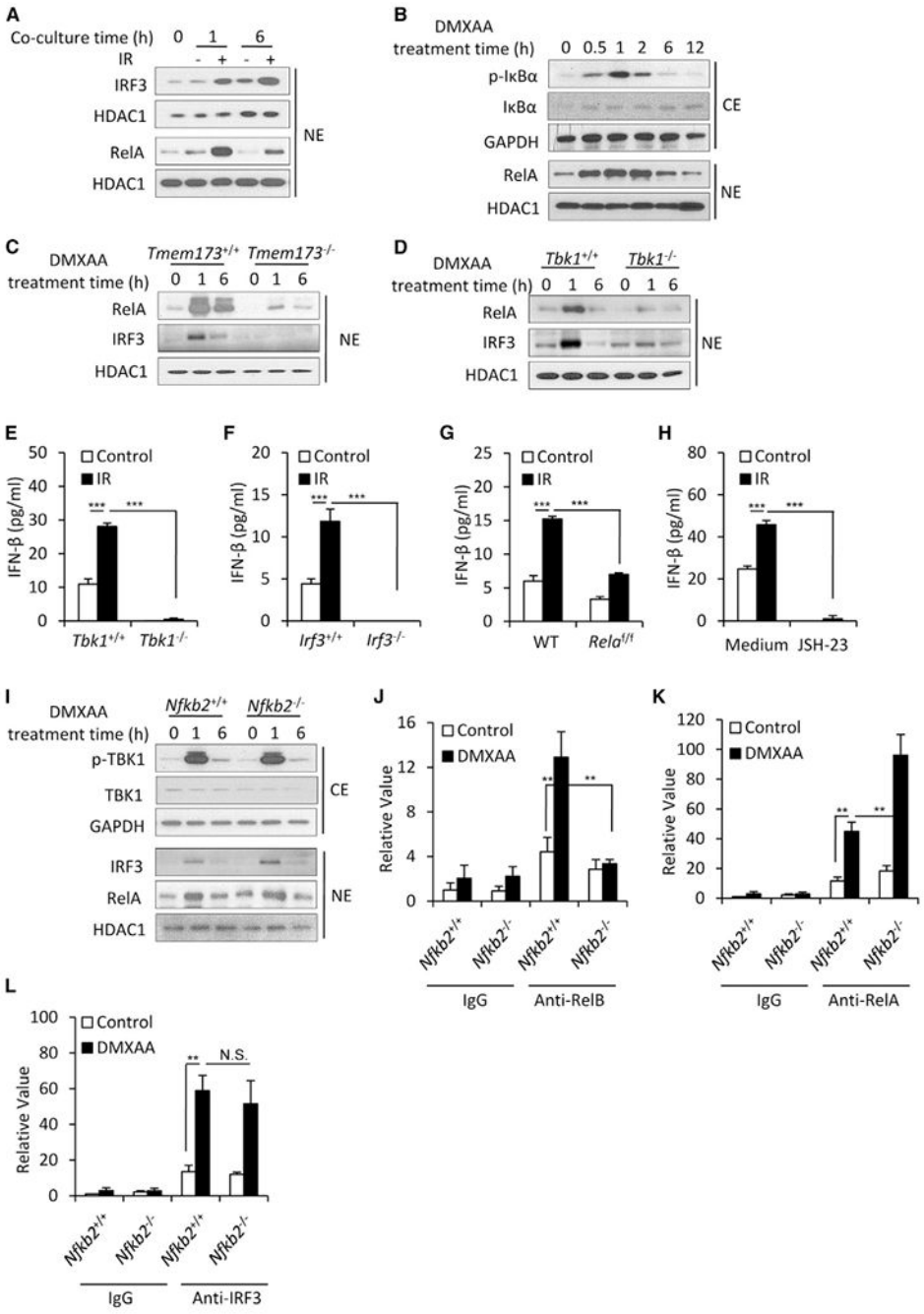

Figure 5. Non-canonical NF-κB Regulates IFN-β Expression through Inhibition of RelA Binding to the *Ifnb* Promoter in DCs

(A) Immuno-blotting analysis of indicated protein in nuclear (NE) extracts of purified BMDCs after co-cultured with irradiated or non-irradiated MC38 cells for indicated time.

(B) Immuno-blotting analysis of indicated phosphorylated (p-) and total protein in cytoplasmic (CE) and nuclear (NE) extracts of BMDCs stimulated with 50 μg/mL DMXAA for indicated time points.

(C) Immuno-blotting analysis of indicated protein in nuclear (NE) extracts of *Tmem17*$^{+/+}$ and *Tmem173*$^{-/-}$ BMDCs stimulated with 50 μg/mL DMXAA for indicated time points.

(D) Immuno-blotting analysis of indicated protein in nuclear (NE) extracts of *Tbk1*$^{+/+}$ and *Tbk1*$^{-/-}$ macrophages stimulated with 50 μg/mL DMXAA for indicated time points.
(E and F) ELISA assay was performed to measure IFN-β produced by *Tbk1*$^{+/+}$ and *Tbk1*$^{-/-}$ macrophages (E) or *Irf3*$^{+/+}$ and *Irf3*$^{-/-}$ BMDCs (E) after co-cultured with irradiated or non-irradiated MC38 cells.
(G) BMDCs were induced with bone marrow cells from WT and *Rela*$^{f/f}$ mice which were treated with 50 μg/mL TAT-Cre for 2 hr. ELISA assay was performed to measure IFN-β produced by TAT-Cre pretreated WT and *Rela*$^{f/f}$ BMDCs after being co-cultured with irradiated or non-irradiated MC38.
(H) ELISA assay was performed to measure IFN-β produced by BMDCs after being co-cultured with irradiated or non-irradiated MC38 cells in absence or presence of 25 μM JSH-23.
(I) Immuno-blotting analysis of indicated phosphorylated (p-) and total protein in cytoplasmic (CE) and nuclear (NE) extracts of *Nfkb2*$^{+/+}$ and *Nfkb2*$^{-/-}$ BMDCs stimulated with 50 μg/mL DMXAA for indicated time points.
(J–L) *Nfkb2*$^{+/+}$ and *Nfkb2*$^{-/-}$ BMDCs were stimulated with 50 μg/mL DMXAA for 2 hr. ChIP assays were performed and quantified by qPCR to detect the binding of RelB (J), RelA (K), and IRF3 (L) to the *Ifnb* promoter. Input DNA was used as an internal control and the data are shown as the relative fold increased over IgG control.
Representative data are shown from three experiments with 3–5 duplicated samples in each group. Data are represented as mean ± SD; **p < 0.01 and ***p < 0.001. Please also see Figure S4.

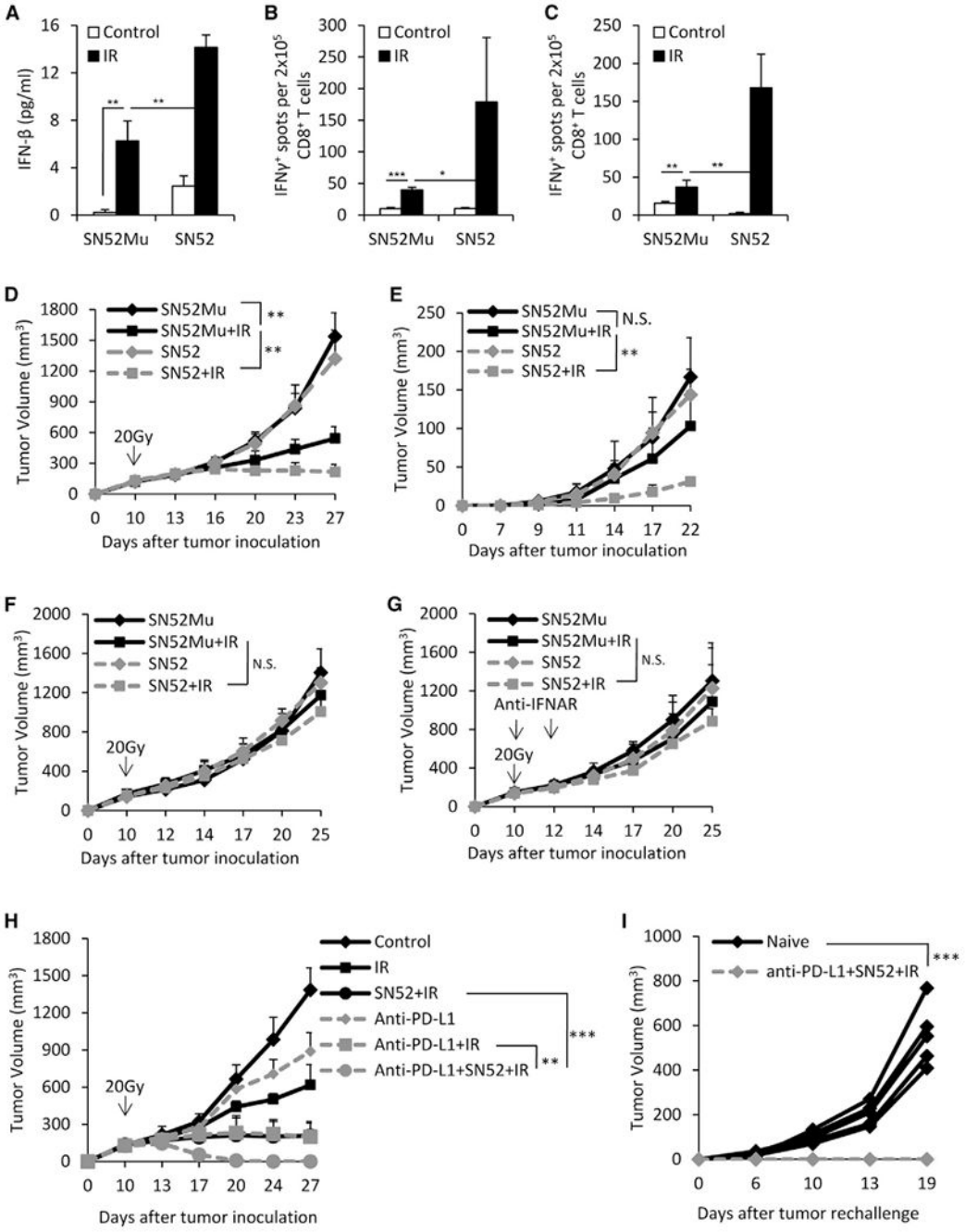

Figure 6. Inhibition of Non-canonical NF-κB Can Promote Radiation-Induced Anti-tumor Immunity

(A) WT BMDCs were pretreated with 40 μg/mL N52Mu or SN52 for 30 min and then co-cultured with irradiated or non-irradiated MC38 cells. ELISA assay wasperformed to measure IFN-β produced by purified BMDCs as described in Figure 3E.

(B and C) MC38-SIY tumors (B) and MC38 tumors (C) established in B6 mice were treated locally with one dose of 20 Gy IR. 40 μg SN52Mu or SN52 was administered i.t. in tumor-bearing mice on day −1, day 1, and day 3 of radiation.

(B) On day 4 post IR, tumors were removed and the cross-priming ability of DCs was evaluated by counting IFN-γ^+ spots as described in Figure 2C.
(C) On day 7 post IR, TDLNs were removed and tumor antigen-specific $CD8^+$ T cell function was measured by ELISPOT assays as described in Figure 2F.
(D) MC38 tumors established in B6 mice were treated with one dose of 20 Gy IR. 40 μg SN52Mu or SN52 was administered i.t. every 2 days for a total of four times staring from 1 day before radiation. Tumor growth was monitored after radiation.
(E) B6 mice were injected s.c. with 1×10^6 MC38 cells on left flank on day 0 (primary tumor) and another 1×10^6 MC38 cells on left flank on day 5 (secondary tumor). On day 10, primary tumors were treated with IR and SN52Mu or SN52 as described in (D). The growth of secondary tumors was monitored after 7 days of inoculation.
(F) MC38 tumors established in *Tmem17*$^{+/+}$ and *Tmem173*$^{-/-}$ mice were treated locally with one dose of 20 Gy IR. 40 μg SN52Mu or SN52 was administered i.t. every 2 days for a total of four times staring from 1 day before radiation. Tumor growth was monitored after radiation.
(G) MC38 tumors established in B6 mice were treated with one dose of 20 Gy IR. 40 μg SN52Mu or SN52 was administered i.t. every 2 days for a total of four times staring from 1 day before radiation. All mice were treated with 200 μg anti-IFNAR1 as described in Figure 3A. Tumor growth was monitored after radiation.
(H) MC38 tumors in B6 mice were established and treated with IR and SN52 as described in (D). On the day of IR, 200 mg anti-PD-L1 (10F.9G2) or isotype control were given by i.p. every 3 days for a total of four times. Tumor growth was monitored after IR.
(I) Thirty days after tumor eradication, tumor-free mice from anti-PD-L1+SN52+IR treatment group were rechallenged with 2×10^6 MC38 cells on the opposite flank. Tumor growth on naive and tumor-free mice was monitored.
Representative data are shown from three experiments (one experiment for F and G) conducted with 4–6 mice in each group. Data are represented as mean ± SD; *$p < 0.05$, **$p < 0.01$, and ***$p < 0.001$. Please also see Figure S5.

KEY RESOURCES TABLE

REAGENT or RESOURCE	SOURCE	IDENTIFIER
Antibodies		
PerCP/Cy5.5 anti-mouse CD3	Biolegend	Cat# 100217, RRID:AB_1595597
PE/Cy7 anti-mouse CD3	BioLegend	Cat# 100220, RRID:AB_1732057
FITC Rat Anti-mouse CD4	BD PharMingen	Cat# 553729, RRID:AB_395013
PE/Cy7 anti-mouse CD4	BioLegend	Cat# 116016, RRID:AB_2563111
APC anti-mouse CD8a	BioLegend	Cat# 100712, RRID:AB_312751
PE anti-mouse CD8a	BioLegend	Cat# 100708, RRID:AB_312747
PerCP/Cy5.5 anti-mouse CD8a	BioLegend	Cat# 100734, RRID:AB_2075238
FITC Rat Anti-mouse CD8a	BD Pharmingen	Cat# 553030; RRID:AB_394568
APC/Cy7 anti-mouse/human CD11b	BioLegend	Cat# 101226, RRID:AB_830642
PerCP/Cy5.5 anti-mouse/human CD11b	BioLegend	Cat# 101228, RRID:AB_893232
PE/Cy7 anti-mouse/human CD11b	BioLegend	Cat# 101216, RRID:AB_312799
APC anti-mouse CD11c	BioLegend	Cat# 117310, RRID:AB_313779
PE/Cy7 anti-mouse CD11c	BioLegend	Cat# 117317, RRID:AB_49356
FITC Anti-mouse CD11c	BioLegend	Cat# 117306, RRID:AB_313775
FITC Anti-mouse CD45.2	BioLegend	Cat# 109806, RRID:AB_313443
APC/Cy7 anti-mouse CD45	BioLegend	Cat# 103116, RRID:AB_312981
PerCP/Cy5.5 anti-mouse CD45.2	BioLegend	Cat# 109828, RRID:AB_893350
Pacific-Blue anti-mouse CD45	BioLegend	Cat# 103126, RRID:AB_493535
PE anti-mouse CD80	BioLegend	Cat# 104707, RRID:AB_313128
Pacific-Blue anti-mouse CD80	BioLegend	Cat# 104724, RRID:AB_2075999
APC/Cy7 anti-mouse CD86	BioLegend	Cat# 105029, RRID:AB_2074993
APC anti-mouse CD86	BioLegend	Cat# 105012, RRID:AB_493342
APC anti-mouse I-A/I-E	BioLegend	Cat# 107614, RRID:AB_313329
Pacific-Blue anti-mouse I-A/I-E	BioLegend	Cat# 107620, RRID:AB_493527
Brilliant Violet 510TM anti-mouse I-A/I-E	BioLegend	Cat# 07635, RRID:AB_2561397
PerCP/Cy5.5 anti-mouse H-2Kb	BioLegend	Cat# 116516, RRID:AB_1967133
Alexa Fluro 488 anti-mouse H-2Kb	BioLegend	Cat# 116510, RRID:AB_492915
NFκB p52 Antibody (C-5) (for co-IP)	Santa Cruz	Cat# sc-7386 X; RRID:AB_2267131
NFκB p52 Antibody (C-5) (for WB)	Santa Cruz	Cat# sc-7386; RRID:AB_2267131
TBK1/NAK Antibody	Cell Signaling	Cat#3013; RRID:AB_10695535
NF-κB Non-Canonical Pathway Antibody Sampler Kit	Cell Signaling	Cat# 4888
Histone Deacetylase 1 (HDAC1) Antibody	Cell Signaling	Cat# 2062; RRID:AB_2118523
GAPDH Antibody	Proteintech Group	Cat# 60004-1-Ig; RRID:AB_2107436
IKKα antibody	Santa Cruz	Cat# sc-7606; RRID:AB_627784
NF-κB Pathway Sampler Kit	Cell Signaling	Cat# 9936
NF-κB p65 (C22B4) Antibody	Cell Signaling	Cat# 4764; RRID:AB_823578

REAGENT or RESOURCE	SOURCE	IDENTIFIER
Phospho-TBK1/NAK (Ser172) (D52C2)	Cell Signaling	Cat# 5483; RRID:AB_10693472
Phospho-IRF-3 (Ser396) (D6O1M)	Cell Signaling	Cat# 29047
IRF-3 (D83B9)	Cell Signaling	Cat# 4302; RRID:AB_1904036
Goat Anti-Mouse IgG (H+L)-HRP Conjugate	Bio-Rad	RRID: AB_11125547
Goat Anti-Rabbit IgG (H+L)-HRP Conjugate	Bio-Rad	RRID: AB_11125143
InVivoMAb anti-mouse PD-L1 (B7-H1)	Bio X Cell	Cat# BE0101, RRID:AB_10949073
nVivoMAb anti-mouse CD8α	Bio X Cell	Cat# BE0004-1, RRID:AB_1107671
InVivoMAb anti-mouse IFNAR-1	Bio X Cell	Cat# BE0241, RRID:AB_2687723
InVivoMAb rat IgG2a isotype control	Bio X Cell	RRID: AB_1107769
Bacterial and Virus Strains		
IFN-β-expressing adenovirus (Ad-IFN-β)	Byron Burnette (Burnette et al., 2011)	N/A
Chemicals, Peptides, and Recombinant Proteins		
Recombinant Mouse GM-CSF Protein	R&D systems	415-ML-010
Cre Recombinase, TAT-Cre	Excellgen	EG-1001
JSH-23	Selleckchem	S7351
ALBUMIN, BOVINE	AMRESCO	0332-100G
DMXAA	SIGMA	D5817-25MG
2′3′-cGAMP	Invivogen	tlrl-cga23
MG-132	Selleckchem	S2619
Critical Commercial Assays		
EasySep Mouse CD8a Positive Selection Kit	STEM CELL	18753
EasySep Mouse CD11c Positive Selection Kit II	STEM CELL	18780
NE-PER Nuclear and Cytoplasmic Extraction Reagents	Thermo Scientific	78833
VeriKine-HS Mouse Interferon Beta Serum ELISA Kit	PBL assay science	42410-2
Magna ChIPTM A/G	Millipore	17-10085
EasySep Mouse T Cell Enrichment Kit	STEM CELL	19751
Pierce Crosslink Magnetic IP/Co-IP Kit	Thermo Scientific	88805
Mouse CXCL10/IP-10/CRG-2 Quantikine ELISA Kit	R&D Systems	MCX100
HA Tag IP/Co-IP Kit	Thermo Scientific	26180
Dynabeads His-Tag Isolation & Pulldown	Invitrogen	10103D
Universal Kinase Activity Kit	R&D systems	EA004
Click-iT Plus EdU Alexa Fluor 647 Flow Cytometry Assay Kit	Thermo Scientific	C10635
Experimental Models: Cell Lines		
MC38	Fu Lab	(Deng et al., 2014b)
MC38-SIY	Fu Lab	(Deng et al., 2014b)
B16-SIY	Fu Lab	PMCID: PMC3927846
Experimental Models: Organisms/Strains		
Mouse: C57BL/6J (WT)	Jackson Laboratory	RRID:IMSR_JAX:000664
Mouse: B6.129S1-Rela^{tm1Ukl}/J (*Rela*$^{f/f}$)	Jackson Laboratory	RRID:IMSR_JAX:024342

REAGENT or RESOURCE	SOURCE	IDENTIFIER
Mouse: B6.Cg-Tg(*Itgax-cre*)1-1Reiz/J	Jackson Laboratory	RRID:IMSR_JAX:008068
Mouse: B6.129P2-Lyz2$^{tm1(cre)Ifo}$/J (*Lyz2-Cre*)	Jackson Laboratory	RRID:IMSR_JAX:004781
Mouse: *Nfkb2*$^{-/-}$	Ulrich Siebenlist	https://doi.org/10.1084/jem.187.2.147
Mouse: *Relb*$^{f/f}$	Falk Weih	https://doi.org/10.4049/jimmunol.167.4.1909
Mouse: *Irf3*$^{-/-}$	T. Taniguchi	PMID: 12821121
Mouse: *Tmem173*$^{-/-}$	Glen N. Barber	https://doi.org/10.1038/nature08476
Mouse: *Chuk*$^{f/f}$	Yinling Hu	https://doi.org/10.1016/j.ccr.2008.07.017
Oligonucleotides		
Primer: *Ifnb* promoter forward: 5′-ATTCCTCTGAGGCAGAAAGGACCA-3′	IDT	N/A
Primer: *Ifnb* promoter forward: 5′-GCAAGATGAGGCAAAGGCTGTCAA-3′	IDT	N/A
Software and Algorithms		
Graphpad Prism 6	GraphPad Software	RRID:SCR_002798
ImageJ	NIH	RRID: SCR_003070
FlowJo v10.3	FlowJo	RRID:SCR_008520
ImmunoSpot 5.0	ImmunoSpot	RRID:SCR_011082
Other		
Peptide: SN52: AAVALLPAVLLALLAPVQRKRRKALP	GenScript	N/A
Peptide: SN52Mu: AAVALLPAVLLALLAPVQRNGRKALP	GenScript	N/A
Vector: pcDNA3.1-6His-TBK1 WT	GenScript	Cat# SC1200 U7841DD090_1
Vector: pcDNA3.1-6His-TBK1 K38A	GenScript	Cat# SC1200M U7841DD090_2
Vector: pcDNA3.1-6His-TBK1 KDD	GenScript	Cat# SC1200M U7841DD090_3
Vector: pcDNA3.1-HA-p100	GenScript	Cat# SC1200 U7841DD090_4